IEEE Access
Multidisciplinary | Rapid Review | Open Access Journal

Received October 18, 2020, accepted October 23, 2020, date of publication October 26, 2020, date of current version November 10, 2020.

Digital Object Identifier 10.1109/ACCESS.2020.3033937

LUT-Based Focal Beamforming System Using 2-D Adaptive Sequential Searching Algorithm for Microwave Power Transfer

JONGSEOK BAE[1], (Member, IEEE), SANG-HWA YI[2], (Member, IEEE), HYUNGMO KOO[1], SUNGJAE OH[1], HANSIK OH[1], WOOJIN CHOI[1], (Graduate Student Member, IEEE), JAEKYUNG SHIN[1], CHAN MI SONG[1], (Member, IEEE), KEUM CHEOL HWANG[1], (Senior Member, IEEE), KANG-YOON LEE[1], (Senior Member, IEEE), AND YOUNGOO YANG[1], (Senior Member, IEEE)

[1]Department of Electrical and Computer Engineering, Sungkyunkwan University, Suwon 16419, South Korea
[2]Department of Electrical Environment Research Center, Korea Electrotechnology Research Institute, Changwon–si 51543, South Korea

Corresponding author: Youngoo Yang (yang09@skku.edu)

This work was supported by the Korea Electrotechnology Research Institute (KERI) Primary Research Program through the National Research Council of Science & Technology (NST) funded by the Ministry of Science and ICT (MSIT) under Grant 20A01010.

ABSTRACT This paper presents a look-up table (LUT)-based focal beamforming system that can effectively transmit RF power up to mid-range distances ($\leq$ 3 m) including when the Rx is in the near-field zones. The Tx elements control and radiate signals for the Rx even at the near-field zone ensuring the received signals are in-phase. Since the proposed system uses a LUT for storing the phase sets of the signals for the Tx elements, it requires only very simple hardware and a very simple adaptive control algorithm compared to conventional retroreflective method. In order to track the moving Rx, a 2-D adaptive sequential searching algorithm is proposed. The system can find the optimum phase set by sequentially searching the phase sets for a pre-determined 2-D area. The LUT of the phase sets are generated using geometric analysis over the entire 2-D area where the Rx could be located. To verify the proposed method, a 5.2 GHz mid-range ($\leq$ 3 m) MPT system composed of a 4 $\times$ 8 Tx array and a 2 $\times$ 3 Rx array was designed and implemented. Using the proposed 2-D adaptive sequential searching algorithm, the optimum phase set for focal beamforming can be quickly found for a given position of the Rx. In our experiments, the results showed an RF power level of 177.8 mW was received at the Rx with a distance of 1 m with a total radiated RF power of 16 W. Since the measured received power levels for various Rx positions agree well with the simulation results, the proposed system was proved to be an excellent candidate for the practical application.

INDEX TERMS Microwave power transfer, look-up table, focal beamforming, 2-D adaptive sequential searching algorithm.

I. INTRODUCTION

With the development of the internet of things (IoT) and wireless sensor networks (WSN) for smart home and smart factory applications, the problem of supplying power to the numerous sensors needed has emerged. Wired charging methods for these sensors are not suitable due to how the sensors tend to be installed. While sensors often rely on batteries for power supply, it becomes very difficult and rather expensive to continuously replace batteries over the device's lifecycle.

Wireless power transfer (WPT) can be used to solve this problem. There are four main methods of providing WPT: magnetic induction, EM resonance, capacitive coupling, and MPT [1]. Magnetic induction and EM resonance methods require coils for both Tx and Rx and have a transmission distance of just a few centimeters. In addition, there are tight alignment requirements between the Tx and Rx coils for high efficiency, this is inconvenient in many applications [2]–[4]. Nevertheless, their ability for high power transmission ($>$ several kW) and high transmission efficiency ($>$ 70%) has fostered a lot of active research and development, especially for applications related to mobile devices, electric vehicles, and biomedical devices [5]–[8].

The associate editor coordinating the review of this manuscript and approving it for publication was Giorgio Montisci.

Since MPT is based on RF radiation, a distance of several meters or even several tens of kilometers can be achieved using beamforming technique [9]–[12]. However, path loss due to high operation frequency can be seriously increased as the transmission distance becomes longer. This path loss can be mitigated by beamforming using massive Tx antenna arrays. Beamforming can be conducted by adjusting the phases and magnitudes of the signals at the Tx elements. The main purpose of beamforming for MPT is so that the EM waves radiated from the Tx antenna elements are combined in-phase at the antenna of the Rx.

For far-field or long-range (more than several meters in general) MPT applications, retrodirective methods have been conventionally used. The Tx for retrodirective systems requires the Rx to have additional antennas to sense the direction of the Rx using the received signal which is transmitted from the Rx [13]–[18]. Then, using the direction of the Rx, the Tx antenna array can form its main beam toward the Rx.

However, for short- or mid-range (less than a few meters in general) MPT applications, a technique that covers application at both far- and near-fields is required. The retroreflective method has been used for such short- or mid-range MPT systems [19]–[22]. To obtain the optimum phase sets for transmitting signals from the Tx elements, the Tx using the retroreflective method needs an additional Rx at each Tx element to receive pilot signals which are transmitted from the Rx. Hence, a Rx is required for the Tx to receive the pilot signal. As a result, any MPT system based on the retroreflective method has very complex Tx and Rx circuits, control circuits to extract the optimum Tx phase set, and additional in-band or out-band communication circuits for signals sent between the Tx and Rx.

In [19], a retroreflective beamforming system using four Tx antenna elements was presented for the 2.08 GHz band. With a total transmitted power of 1 W, 0.25 W per antenna, RF power of 14 mW was received at a distance of 0.5 m through a single Rx antenna. In [20], a distributed retroreflective beamforming system using eight Tx antenna elements was reported for the 2.125 GHz frequency band. With a total transmitted power of 1.4 W, 0.175 W per antenna, RF power of 7 mW was received at a distance of 0.5 m through a single Rx antenna. In [21], a retroreflective beamforming system using 16 Tx antenna elements and 8 Rx antenna elements was reported for the 2.45 GHz frequency band. The received power was improved by adaptively adjusting the number of rectennas in the Rx using the calculated size of the focal point in the near-field zone. By transmitting 250 mW, dc power of about 10 mW was obtained through three rectennas at a distance of 1 m. In [22], a retroreflective beamforming system using 64 Tx antenna elements and 6 Rx antenna elements was reported for the 5.2 GHz frequency band. A new calibration method was proposed to calculate the phase offsets for the unit's Tx and Rx circuits in the Tx.

Especially, for fixed near-field positions, a focused antenna array can effectively transmit RF energy to an Rx [23]–[30]. The optimum phase sets for the multiple Tx antennas are implemented at each Tx element to focus the beam at the point where the Rx is located. In [29], a focused antenna array with 64 Tx antenna elements and 16 Rx antenna elements were reported for the 5.8 GHz frequency band. The phases for the Tx antenna elements were controlled using different lengths of the transmission lines at the inputs of the antennas. For a total transmitted power of 100 mW, RF power levels of 19.9 and 33.2 mW received by an Rx at a fixed point 40 cm away were reported using a conventional far-field beamforming method and a focused antenna array method, respectively. In [30], a focused antenna array 1×1 m^2 in size for the Tx and Rx antennas was used in the 5.8 GHz frequency band. The phases of the Tx antenna elements were controlled using different lengths of the coaxial transmission lines at the inputs of the antennas. For a total transmitted power of 500 W, received RF power levels of 164.89 and 209.26 W for the Rx at a fixed point with a distance of 10 m were reported using a conventional far-field beamforming method and the focused antenna array method, respectively. The above results show that a focused antenna array can be an effective alternative for short- and mid-range MPT including the near-field zone. However, for most MPT applications that involve a moving Rx, for acceptable performance these system need to have the ability to quickly find the optimum phase sets for the Tx signals and to adaptively control the phases of the signals of the Tx elements according to the changing position of the Rx.

In this paper, an LUT-based adaptive focal beamforming system is proposed for short- or mid-range (≤ 3 m, including the near-field zone) MPT applications. The LUT contains the optimum phase sets, extracted for the Tx elements, to focus the beam at each position in a 2-D zone where the Rx could be located. The proposed MPT system is designed to find the optimal phase set among the pre-stored sets in the LUT and to apply it to the Tx using a 2-D adaptive sequential searching algorithm based on the received power from the Rx. Compared to the retroreflective method which finds and sets the optimum phase for each Tx element in a one-by-one manner in the control domain, the proposed method may well be much faster by finding and setting the optimal phase set at one time for all the Tx elements. In addition, the hardware complexity of the proposed method becomes a lot lower than that of the retroreflective method.

To verify the proposed method, an LUT-based focal beamforming system equipped with a 4×8 Tx array and 2×3 Rx antennas was designed and implemented for the 5.2 GHz frequency band. Each element of the Tx array radiates RF power of 0.5 W through a patch antenna and has an embedded micro-controller unit (MCU) for running the beamforming algorithm. Measurement results according to various Rx positions in the mid-range (≤ 3 m) including the near-field zone will be presented with the simulation results.

II. LUT-BASED FOCAL BEAMFORMING

Fig. 1 shows a conceptual diagram of the LUT-based focal beamforming system using an M×N Tx antenna array and K×L focal points where the Rx could be located. The opti-

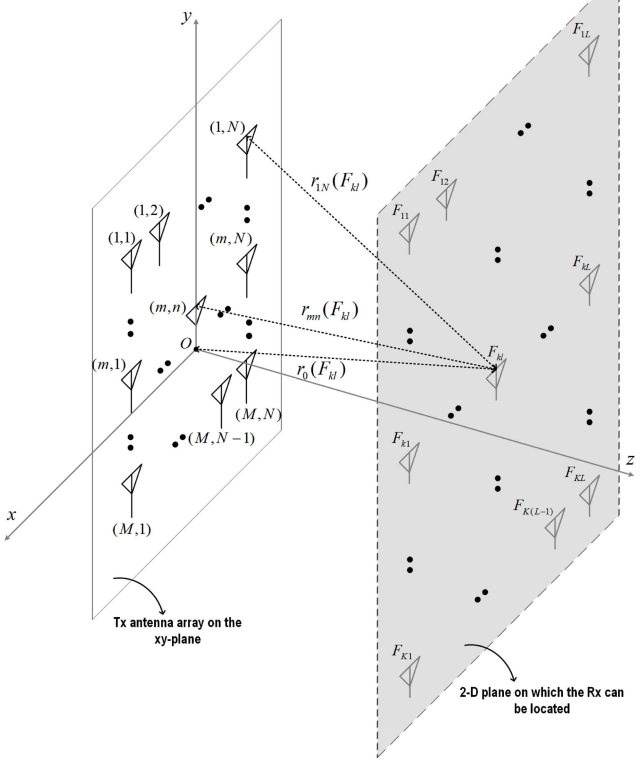

FIGURE 1. Conceptual diagram of the LUT-based focal beamforming system composed of M×N Tx antenna array.

mum phase set for a Tx element can be calculated using a geometric method. The path difference between the distance from the origin to the the (k,l)-th focal point (F_{kl}) and the distance from the (m,n)-th Tx antenna element to the F_{kl} can be translated as a relative phase difference of $(\theta_{mn}(F_{kl}))$ as follows.

$$\theta_{mn}(F_{kl}) = \frac{2\pi}{\lambda_0}(r_{mn}(F_{kl}) - r_0(F_{kl})), \tag{1}$$

where λ_0 is the wavelength in free space, $r_{mn}(F_{kl})$ is the distance between the (m,n)-th Tx antenna element and the focal point (F_{kl}), and $r_0(F_{kl})$ is the distance between the origin and the focal point (F_{kl}). The position of the (m,n)-th Tx antenna array can be expressed as $(x_{mn},y_{mn},0)$ in Cartesian coordinates, while the (k,l)-th focal point (F_{kl}) can be expressed as (x_{kl},y_{kl},z_{kl}). Then, (1) can be rewritten as:

$$\theta_{mn}(F_{kl}) = \frac{2\pi}{\lambda_0}\sqrt{(x_{mn}-x_{kl})^2+(y_{mn}-y_{kl})^2+(z_{mn}-z_{kl})^2} - \sqrt{x_{kl}^2+y_{kl}^2+z_{kl}^2}, \tag{2}$$

The relative phase difference of $\theta_{mn}(F_{kl})$ can be used as the phase to control the (m,n)-th Tx element for a focal point of F_{kl} that compensates for the relative path difference. Therefore, the conditions for optimal focal beamforming at

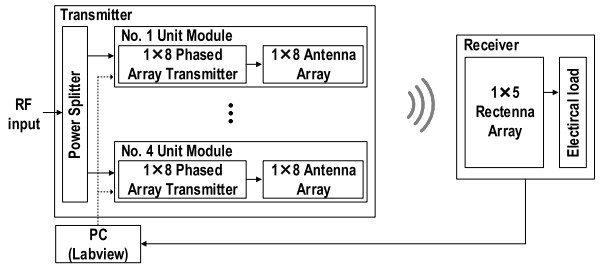

FIGURE 2. Block diagram of the proposed LUT-based focal beamforming system.

the (k,l)-th focal point can be expressed using a M×N phase matrix as follows.

$$\Theta_{Tx,opt}(F_{kl}) = \begin{bmatrix} \theta_{11}(F_{kl}) & \cdots & \theta_{1N}(F_{kl}) \\ \vdots & \ddots & \vdots \\ \theta_{M1}(F_{kl}) & \cdots & \theta_{MN}(F_{kl}) \end{bmatrix}, \tag{3}$$

where $\Theta_{Tx,opt}(F_{kl})$ are the optimum phase sets for the M×N Tx antenna elements, this allows the system to perform optimal focal beamforming to the (k,l)-th focal point. The LUT has a K×L number of the M×N phase matrices $(\Theta_{Tx,opt})$ for the K×L focal points at the Rx. To adaptively focus the beam at the moving Rx, an adaptive control algorithm and a control system to find the optimal phase set among the K×L phase matrices stored in the LUT are required to maximize the received power at the Rx.

It would be possible to extract LUTs for multiple planes that cover the entire possible set of 3-D positions of the Rx. But for the limited range between the Tx and Rx, simply using an LUT for a plane with a fixed z can be rather effective by making the system and the adaptive beamforming algorithm simpler. In this work, the LUT was extracted at a single plane of the focal points with a fixed z of 1.0 m. To demonstrate the beam focusing ability of the proposed short-range WPT system with sufficient angular resolution, a square zone of 1.0×1.0 m^2 for 13×13 individual focal points was selected to extract the LUT.

III. SYSTEM DESIGN AND IMPLEMENTATION

A. SYSTEM DESIGN

For the proposed LUT-based focal beamforming system, a Tx composed of a massive antenna array and an Rx composed of a rectenna array for the 5.2 GHz frequency band were designed. Fig. 2 shows the block diagram of the proposed LUT-based focal beamforming system. The Rx consists of a 1×5 rectenna array that receives RF signals and converts them from RF to dc. A voltage doubler based on single-stage class-F structure was applied to maximize the conversion efficiency [31]. A 2-section input matching network for the individual rectifier based on a series transmission line and an open stub was designed for class-F operation and fundamental impedance matching. The individual rectifier used in the 1×5 rectenna array exhibited an efficiency of 64.1% and an output dc voltage of 5.1 V at an input power of 24 dBm in 5.2 GHz frequency band. The dc outputs of the 1×5 rectenna array were directly combined in current and supplied

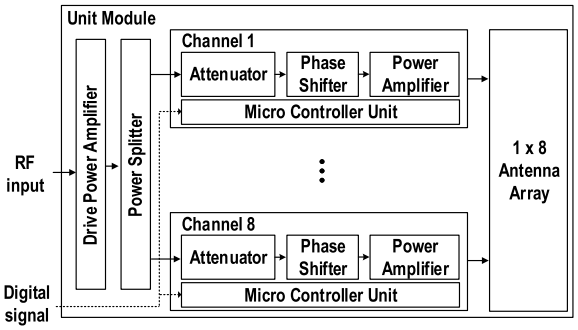

FIGURE 3. Block diagram of the unit Tx module.

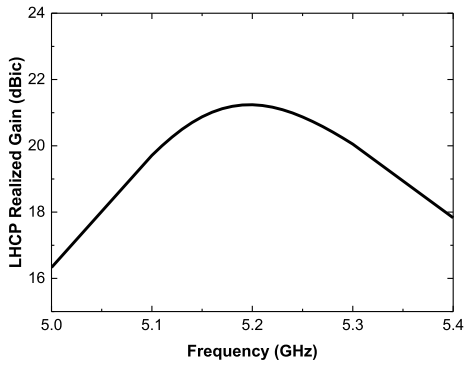

(a)

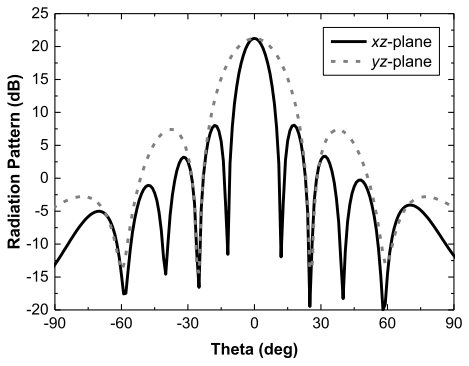

(b)

FIGURE 4. Simulated results of the Tx antenna array: (a) gain, (b) beam patterns.

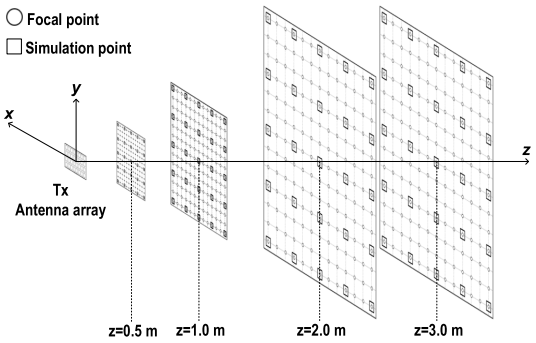

FIGURE 5. Simulation setup for received power.

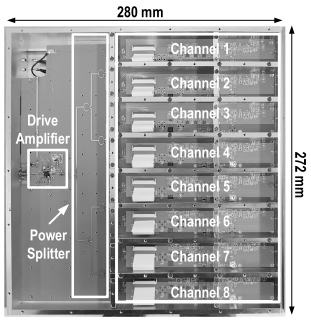

(a)

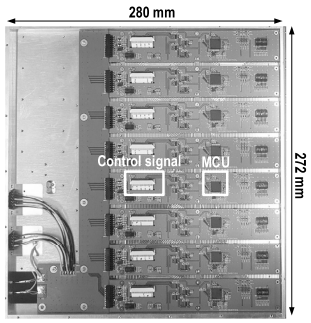

(b)

FIGURE 6. Photograph of the implemented Tx unit module: (a) top view, (b) bottom view.

as electrical load. The received RF power was measured using an additional antenna in the Rx and a spectrum analyzer. The measured power is to be recorded on a PC in order to run the 2-D adaptive sequential searching algorithm for optimum focal beamforming. For the Rx antenna, a trimmed rectangular patch with left-handed circular polarization (LHCP) was designed on an RF-35 substrate with a thickness of 1.52 mm, a dielectric constant of 3.5, and a loss tangent of 0.0018. The width and length of the substrate for the unit antenna are 35.85 mm (0.62 λ_0) and 45 mm (0.78 λ_0), respectively. In the broadside direction, the LHCP antenna exhibited a gain of 6.563 dBic.

The 4 $\times$ 8 Tx array is composed of four 1 $\times$ 8 unit modules. The RF input power is amplified using a drive power amplifier and is distributed to the four unit modules using a Wilkinson power splitter. A 1 $\times$ 8 unit module includes 8 Tx elements with 8 antennas. The Tx element was designed to include a drive power amplifier, a 1:8 Wilkinson power splitter, an attenuator, a phase shifter, power amplifier, and an internal MCU to control the attenuator and the phase shifter, as shown in Fig. 3. The 1:8 Wilkinson power splitter was designed to be used on the RF-35 substrate. The 6-bit digital attenuator has an LSB of 0.5 dB, and a maximum attenuation of 31.5 dB. The 6-bit digital phase shifter has an LSB of 5.625° and a phase coverage of 360°. The drive and power amplifiers have a power gain of 32 dB and a P1dB of 32 dBm. For the Tx antenna, a patch based on the Koch-curved rectangular structure for LHCP was implemented on the same RF-35 substrate [22]. In the broadside direction, a single Tx antenna exhibited a gain of 6 dBic. The width and length of the square substrate used for a single antenna is

TABLE 1. Component list used in the unit Tx module.

Name	Part nubmer	Features
Phase shifter	HMC1133LP5E	360° coverage, LSB= 5.625°
Attenuator	HMC1122LP4ME	0.5 dB LSB steps to 31.5 dB
Power amplifer	SE5003L1-R	P1dB: 32 dBm Power gain: 32 dB
MCU	STM32F103R4T6A	UART, USB 2.0 interface

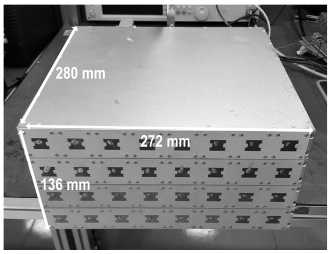

(a)

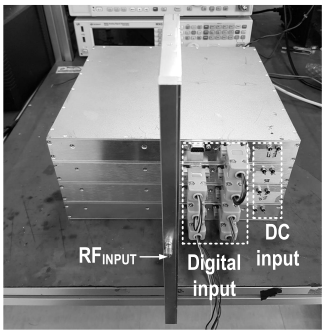

(b)

FIGURE 7. Photograph of the implemented Tx: (a) front view, (b) rear view.

34 mm (0.59 λ_0). Since the gain of a single Tx antenna is 6 dBic, the gain of the total 4 × 8 antenna array can be approximated as about 21 dBic as shown in Fig. 4a and b.

B. 2-D ADAPTIVE SEARCHING ALGORITHM

Since a LUT extracted from a single plane ($z = 1.0$ m) of 13 × 13 focal points will be used, a 2-D search of the optimum phase matrix would be very effective. If the LUT would be extracted from multiple planes, a 3-D searching algorithm is a simple extension of the proposed 2-D algorithm could be applied. The operation principle of the proposed 2-D searching algorithm is very simple. The algorithm starts with the LUT that has 13 × 13 phase matrices. Each phase matrix is assigned for a position of the focal point and has 4 × 8 elements each of which is assigned to the respective Tx elements. The proposed 2-D sequential searching algorithm works as follows. It sets an initial phase matrix for the Tx with LUT(k,l), where LUT(k,l) indicates the phase matrix for the (k,l)-th focal point. The algorithm consists of searches in the horizontal (x) and vertical (y) axes. First, the algorithm begins with the search in the horizontal axis with LUT(k,l).

The procedure for the search in the horizontal axis is as follows. The received power levels with LUT($k-1$,l), LUT(k,l), and LUT($k+1$,l) are recorded, where LUT(k,l) is the current LUT. If the power with LUT(k,l) among the three measured power levels is highest, the algorithm jumps to search in the vertical axis. Else if the power with either LUT($k+1$,l) or LUT($k-1$,l) is highest, the LUT with the highest power is set as the current LUT i.e., LUT(k,l). Then, the search in the horizontal axis is repeated.

The procedure for search in the vertical axis is as follows. The received power levels with LUT(k,$l-1$), LUT(k,l), and LUT(k,$l+1$) are recorded, where LUT(k,l) is the current LUT. If the power with LUT(k,l) among the three measured power levels is highest, the algorithm jumps to search in the horizontal axis. Else if the power with either LUT (k,$l-1$) or LUT(k,$l+1$) is highest, the LUT with the highest power is set as the current LUT i.e., LUT(k,l). Then, the search in the vertical axis is repeated.

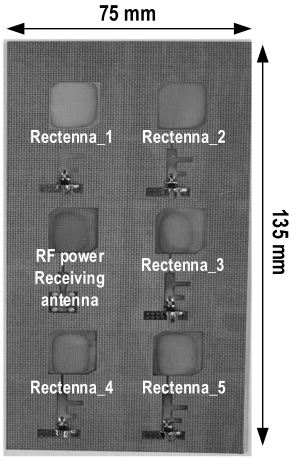

FIGURE 8. Photograph of the implemented Rx.

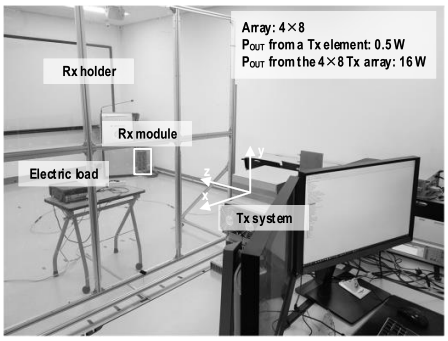

FIGURE 9. Experimental setup for the LUT-based focal beamforming system.

C. SIMULATION FOR THE RECEIVED POWER

The received power for the various Rx positions was simulated using the LUT generated for the multiple planes with fixed z. Fig. 5 shows the simulation setup for the received power which illustrates the grid of focal points and the simulated points on the same plane. The sizes of the planes for the focal points were calculated by considering the azimuthal angle and elevation angle from the Tx for each focal plane. Using (3), four LUTs were generated from four square zones

TABLE 2. Measured and simulated received RF power levels at the Rx.

Rx location (m)		z:1.0			z:2.0			z:3.0		
		x:−0.4 y:0.4	x:−0.2 y:0.2	x:0.0 y:0.0	x:−1.0 y:1.0	x:−0.5 y:0.5	x:0.0 y:0.0	x:−1.0 y:1.0	x:−0.5 y:0.5	x:0.0 y:0.0
RF power levels	Simulation (dBm)	19.6	22.0	22.7	10.7	14.5	16.8	10.5	12.6	13.3
	Measurement (dBm)	18.6	21.2	22.5	10.1	13.5	16.0	9.0	12.5	12.8
dc power levels	Measurement (mW)	98.5	136.9	191.1	9.6	22.2	43.2	9.4	15.3	14.3

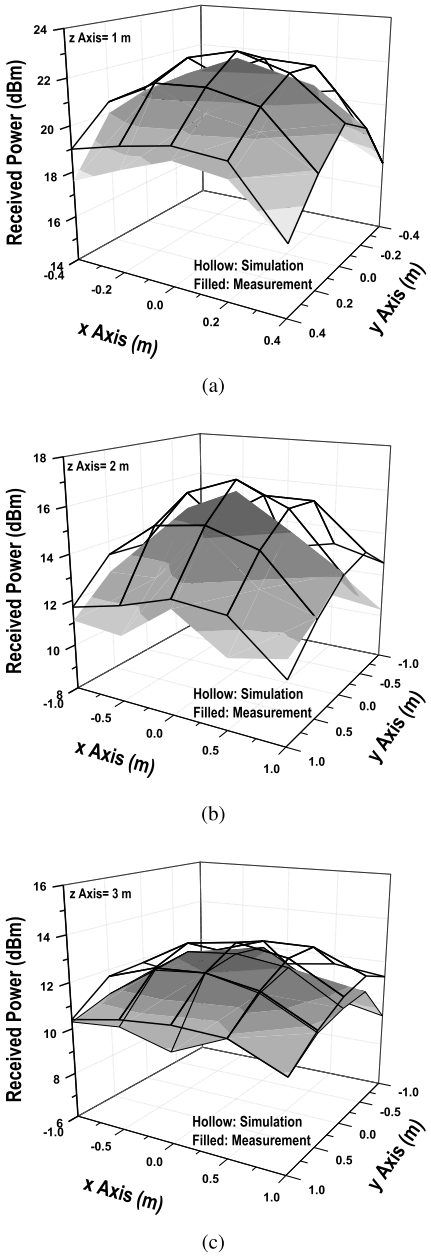

FIGURE 10. Measured and simulated received RF power levels for the various positions of the Rx: (a) z of 1 m, (b) z of 2 m, (c) z of 3 m.

with a fixed z of 0.5, 1.0, 2.0, and 3.0 m. The LUT consists of a 13 × 13 phase matrix for each focal plane. The simulation was performed using CST.

D. IMPLEMENTATION

Fig. 6 shows photographs of the top view (in (a)) and bottom view (in (b)) of an implemented Tx unit module. The size of the implemented unit module is 272 × 280 × 34 mm^3. The top side of the unit module consists mainly of RF circuits, while the bias and digital circuits are implemented on the bottom side. The phase and magnitude of the RF signals supplied to the antenna array are adjusted using the digital circuit. Table 1 shows the component list used in the unit module.

Fig. 7 shows the photographs of the implemented 4 × 8 (four 1 × 8) Tx array: a front view in (a) and a rear view in (b). The implemented Tx has total dimensions of 272 × 280×136 mm^3. The external RF input power is split using a Wilkinson power splitter and is applied to the four unit modules. Fig. 8 shows a photograph of the implemented Rx. The size of the Rx is 75×135 × 15.2 mm^3. The RF-dc converters are implemented using Schottky diodes, HSMS286C.

IV. EXPERIMENTAL RESULTS

Fig. 9 shows the experimental setup for the LUT-based focal beamforming system. An Rx holder with a size of 2 × 2 m^2 was fabricated to move the Rx to various positions. A signal generator was used to provide the input RF signal. The 2-D sequential searching algorithm was implemented in a PC using Labview. Among the 6 Rx antennas, 5 Rx antennas were used as rectennas to obtain dc power, while one antenna was used to detect the received RF power, this data is then used to run the 2-D adaptive sequential searching algorithm.

Using the experimental setup shown in Fig. 9, adaptive focal beamforming was performed using the 2-D adaptive sequential searching algorithm for various Rx positions. Each Tx antenna transmitted 0.5 W, which results in a total transmitted power of 16 W with the 4 × 8 array. Fig. 10 shows the 3-D contours of the received RF power levels for the various positions of the Rx. Table 2 shows the measured and simulated RF and dc power levels. Received RF power levels of 22.5, 21.2, and 18.6 dBm were obtained in measurements at Rx positions of (0,0,1), (−0.2,0.2,1), and (−0.4,0.4,1), respectively. The table also shows the measured dc power levels using the 5 rectennas and the electrical load at the Rx. The measured dc power levels of 191.1 mW, 136.9 mW, and 98.5 mW were obtained at the Rx positions of (0,0,1), (−0.2,0.2,1), and (−0.4,0.4,1), respectively. Even at the Rx

TABLE 3. Performance comparison with previous work.

Ref.	Frequency (GHz)	Beamforming Technique	# of Tx array	P_T (W)	# of Rx antennas	P_R (mW)	Distance (m)
[18]	5.8	LUT	16	1.3	16	7* (RF)	0.5
[19]	2.08	Retroreflective	4	1	1	14 (RF)	0.5
[20]	2.125	Retroreflective	8	1.4	1	7 (RF)	0.5
[21]	2.45	Retroreflective	16	0.25	3	11 (RF)	1
[22]	5.2	Retroreflective	64	32	1	8∼446 (RF)	1–4
					5	20∼575 (dc)	1–4
This work	5.2	LUT-based adaptive focal beamforming	32	16	1	9∼177.8 (RF)	1–3
					5	9.4∼191.1 (dc)	1–3

*: Graphically estimated

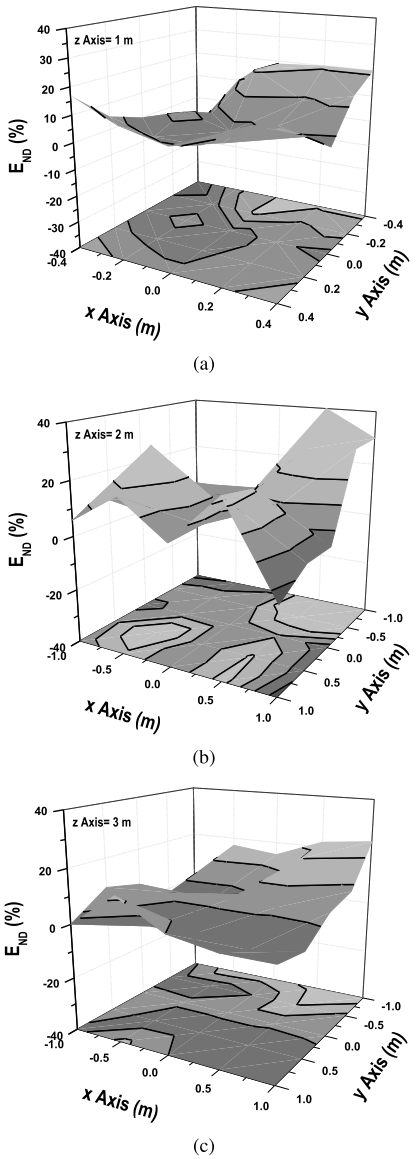

FIGURE 11. Normalized distance error for the various positions of the Rx: (a) *z* of 1 m, (b) *z* of 2 m, (c) *z* of 3 m.

position of (0,0,3), a distance of 3 m, a measured dc power level of 14.3 mW was obtained, this could be sufficient to charge some low-power sensors.

Fig. 11 shows the 3-D contours of the normalized distance errors (E_{ND}'s) for the various positions of the Rx. E_{ND} is defined as follows.

$$E_{ND} = \frac{r_0'(F_{kl}) - r_0(F_{kl})}{r_0(F_{kl})}, \tag{4}$$

where $r_0(F_{kl})$ is a distance between the Tx and Rx for (k,l)-th focal point which was originally set for the measurements. $r_0'(F_{kl})$ is a calculated distance between the Tx and a virtual position of the Rx for (k,l)-th focal point. The virtual position of the Rx is the position where the Rx can receive the same power using the simulation with the measured received power.

There are small mismatches between the simulated and measured results, which can be explained as follows. First, the full-wave simulation using CST Studio Suite was performed in an ideal situation where the transmitting and receiving antennas exist in free space. However, since the actual experiment was conducted in a cavity environment with several scattering bodies around (as shown in Fig. 9), the effect of multiple scattering can be reflected to the measurement results. Second, errors can occur due to the geometric mismatch between the transmitting and receiving antennas. The relative position between the transmitting and receiving antennas in the measurement may be slightly different when compared to the accurate values set in the simulation. Since the measurement results are slightly different from the simulation results, the proposed LUT-based focal beamforming system is proved to be effective and practical.

Table 3 includes a performance summary of this work and compares our results to previous works. Compared to conventional retroreflective systems, the proposed MPT system has a very simple structure. The proposed LUT-based focal beamforming system equipped with a 4×8 Tx antenna array and Rx array achieved high received power levels in various Rx positions by using an 2-D adaptive sequential searching algorithm.

V. CONCLUSION

In this paper, an LUT-based focal beam focusing system using a 2-D adaptive sequential searching algorithm was proposed for short- or mid-range (≤3 m, including near-field zones) MPT applications. Using the proposed methods based on an LUT and a focused antenna array, fast adaptive focal beamforming with relatively simple hardware compared to conventional retroreflective methods was achieved for moving Rx's in the near-field zone. The LUT is composed of phase sets

for the Tx antenna elements for a given 2-D zone somewhere in which the Rx array could be located. Each phase set for the LUT was calculated using a geometric method based on the distances between each Tx antenna element and the focal point.

For verification of the proposed method, a 4×8 Tx array and an Rx array for the 5.2 GHz band were designed and implemented. The 4×8 Tx array was composed of four unit modules. Each 1×8 unit module consists of 8 active phased arrays and 8 antenna elements. Each Tx element of a unit module consists of a digital attenuator, a phase shifter, power amplifiers, and an MCU. A 2-D sequential searching algorithm was implemented with a PC using Labview. The size of the implemented 4×8 Tx array is $272 \times 280 \times 136$ mm^3. The total radiated power from the Tx was 16 W, while the received dc power was 191.1 mW using 5 rectennas at a distance of 1 m. The measured and simulated received power levels for the various positions of the Rx were in good agreement with simulation results, the results prove that the proposed adaptive focal beamforming method is very effective and excellent candidate for practical MPT applications with short- and mid-ranges. Compared to the conventional retroreflective method, the proposed system has significantly compact circuits with a limited range of operation.

REFERENCES

[1] Z. Popovic, "Near-and far-field wireless power transfer," in *Proc. 13th Int. Conf. Adv. Technol., Syst. Services Telecommun. (TELSIKS)*, Nis, Serbia, 2017, pp. 3–6, doi: 10.1109/TELSKS.2017.8246215.

[2] A. Kurs, A. Karalis, R. Moffatt, J. D. Joannopoulos, P. Fisher, and M. Soljacic, "Wireless power transfer via strongly coupled magnetic resonances," *Sci.*, vol. 317, no. 5834, p. 83–86, Jul. 2007, doi: 10.1126/science.1143254.

[3] S. Y. R. Hui, W. Zhong, and C. K. Lee, "A critical review of recent progress in mid-range wireless power transfer," *IEEE Trans. Power Electron.*, vol. 29, no. 9, pp. 4500–4511, Sep. 2014, doi: 10.1109/TPEL.2013.2249670.

[4] T. Arakawa, S. Goguri, J. V. Krogmeier, A. Kruger, D. J. Love, R. Mudumbai, and M. A. Swabey, "Optimizing wireless power transfer from multiple transmit coils," *IEEE Access*, vol. 6, pp. 23828–23838, 2018, doi: 10.1109/ACCESS.2018.2825290.

[5] S. Li and C. C. Mi, "Wireless power transfer for electric vehicle applications," *IEEE J. Emerg. Sel. Topics Power Electron.*, vol. 3, no. 1, pp. 4–17, Mar. 2015, doi: 10.1109/JESTPE.2014.2319453.

[6] C. Cai, J. Wang, Z. Fang, P. Zhang, M. Hu, J. Zhang, L. Li, and Z. Lin, "Design and optimization of load-independent magnetic resonant wireless charging system for electric vehicles," *IEEE Access*, vol. 6, pp. 17264–17274, 2018, doi: 10.1109/ACCESS.2018.2810128.

[7] A. N. Abdulfattah, C. C. Tsimenidis, B. Z. Al-Jewad, and A. Yakovlev, "Performance analysis of MICS-based RF wireless power transfer system for implantable medical devices," *IEEE Access*, vol. 7, pp. 11775–11784, 2019, doi: 10.1109/ACCESS.2019.2891815.

[8] N. Ha-Van and C. Seo, "Modeling and experimental validation of a butterfly-shaped wireless power transfer in biomedical implants," *IEEE Access*, vol. 7, pp. 107225–107233, 2019, doi: 10.1109/ACCESS.2019.2933260.

[9] W. C. Brown, "The history of power transmission by radio waves," *IEEE Trans. Microw. Theory Techn.*, vol. MTT-32, no. 9, pp. 1230–1242, Sep. 1984, doi: 10.1109/TMTT.1984.1132833.

[10] N. Shinohara, "Power without wires," *IEEE Microw. Mag.*, vol. 12, no. 7, pp. S64–S73, Dec. 2011, doi: 10.1109/MMM.2011.942732.

[11] A. Massa, G. Oliveri, F. Viani, and P. Rocca, "Array designs for long-distance wireless power transmission: State-of-the-art and innovative solutions," *Proc. IEEE*, vol. 101, no. 6, pp. 1464–1481, Jun. 2013, doi: 10.1109/JPROC.2013.2245491.

[12] B. Strassner and K. Chang, "Microwave power transmission: Historical milestones and system components," *Proc. IEEE*, vol. 101, no. 6, pp. 1379–1396, Jun. 2013, doi: 10.1109/JPROC.2013.2246132.

[13] S. Komatsu, K. Katsunaga, R. Ozawa, K. Komurasaki, and Y. Arakawa, "Power transmission to a micro aerial vehicle," in *Proc. AIAA Paper*, 2007, p. 1003, doi: 10.2514/6.2007-1003.

[14] Y. Homma, T. Sasaki, K. Namura, F. Sameshima, T. Ishikawa, H. Sumino, and N. Shinohara, "New phased array and rectenna array systems for microwave power transmission research," in *Proc. IMWS-IWPT*, Uji, Kyoto, 2011, pp. 59–62, doi: 10.1109/IMWS.2011.5877091.

[15] S. Nako, K. Okuda, K. Miyashiro, K. Komurasaki, and H. Koizumi, "Wireless power transfer to a microaerial vehicle with a microwave active phased array," *Int. J. Antennas Propag.*, vol. 2014, pp. 1–5, Jan. 2014, doi: 10.1155/2014/374543.

[16] T. Takahashi, T. Sasaki, Y. Homma, S. Mihara, K. Sasaki, S. Nakamura, K. Makino, D. Joudoi, K. Ohashi, "Phased array system for high efficiency and high accuracy microwave power transmission," in *Proc. IEEE Int. Phased Array Syst. Technol. Symp.*, Waltham, MA, USA, Oct. 2016, pp. 1–7, doi: 10.1109/ARRAY.2016.7832563.

[17] N. Shinohara, "Beam control technologies with a high-efficiency phased array for microwave power transmission in japan," *Proc. IEEE*, vol. 101, no. 6, pp. 1448–1463, Jun. 2013, doi: 10.1109/JPROC.2013.2253062.

[18] D. Belo, D. C. Ribeiro, P. Pinho, and N. Borges Carvalho, "A selective, tracking, and power adaptive far-field wireless power transfer system," *IEEE Trans. Microw. Theory Techn.*, vol. 67, no. 9, pp. 3856–3866, Sep. 2019, doi: 10.1109/TMTT.2019.2913653.

[19] X. Wang, S. Sha, J. He, L. Guo, and M. Lu, "Wireless power delivery to low-power mobile devices based on retro-reflective beamforming," *IEEE Antennas Wireless Propag. Lett.*, vol. 13, pp. 919–922, 2014, doi: 10.1109/LAWP.2014.2322493.

[20] J. He, X. Wang, L. Guo, S. Shen, and M. Lu, "A distributed retroreflective beamformer for wireless power transmission," *Microw. Opt. Technol. Lett.*, vol. 57, no. 8, p. 1873–1876, Aug. 2015, doi: 10.1002/mop.29209.

[21] S.-T. Khang, D.-J. Lee, I.-J. Hwang, T.-D. Yeo, and J.-W. Yu, "Microwave power transfer with optimal number of rectenna arrays for midrange applications," *IEEE Antennas Wireless Propag. Lett.*, vol. 17, no. 1, pp. 155–159, Jan. 2018, doi: 10.1109/LAWP.2017.2778507.

[22] H. Koo, Y. Yang, J. Bae, W. Choi, H. Oh, H. Lim, J. Lee, C. Song, K. Lee, and K. Hwang, "Retroreflective transceiver array using a novel calibration method based on optimum phase searching," *IEEE Trans. Ind. Electron.*, early access, Feb. 20, 2020, doi: 10.1109/TIE.2020.2973903.

[23] M. Bogosanovic and A. G. Williamson, "Microstrip antenna array with a beam focused in the near-field zone for application in noncontact microwave industrial inspection," *IEEE Trans. Instrum. Meas.*, vol. 56, no. 6, pp. 2186–2195, Dec. 2007, doi: 10.1109/TIM.2007.907954.

[24] D. R. Smith, V. R. Gowda, O. Yurduseven, S. Larouche, G. Lipworth, Y. Urzhumov, and M. S. Reynolds, "An analysis of beamed wireless power transfer in the fresnel zone using a dynamic, metasurface aperture," *J. Appl. Phys.*, vol. 121, no. 1, Jan. 2017, Art. no. 014901, doi: 10.1063/1.4973345.

[25] L. Shan and W. Geyi, "Optimal design of focused antenna arrays," *IEEE Trans. Antennas Propag.*, vol. 62, no. 11, pp. 5565–5571, Nov. 2014, doi: 10.1109/TAP.2014.2357421.

[26] A. Buffi, P. Nepa, and G. Manara, "Design criteria for near-field-focused planar arrays," *IEEE Antennas Propag. Mag.*, vol. 54, no. 1, pp. 40–50, Feb. 2012, doi: 10.1109/MAP.2012.6202511.

[27] A. Buffi, A. A. Serra, P. Nepa, H.-T. Chou, and G. Manara, "A focused planar microstrip array for 2.4 GHz RFID readers," *IEEE Trans. Antennas Propag.*, vol. 58, no. 5, pp. 1536–1544, May 2010, doi: 10.1109/TAP.2010.2044331.

[28] R. Siragusa, P. Lemaitre-Auger, and S. Tedjini, "Tunable near-field focused circular phase-array antenna for 5.8-GHz RFID applications," *IEEE Antennas Wireless Propag. Lett.*, vol. 10, pp. 33–36, 2011, doi: 10.1109/LAWP.2011.2108632.

[29] V. R. Gowda, O. Yurduseven, G. Lipworth, T. Zupan, M. S. Reynolds, and D. R. Smith, "Wireless power transfer in the radiative near field," *IEEE Antennas Wireless Propag. Lett.*, vol. 15, pp. 1865–1868, 2016, doi: 10.1109/LAWP.2016.2542138.

[30] X. Yi, X. Chen, L. Zhou, S. Hao, B. Zhang, and X. Duan, "A microwave power transmission experiment based on the near-field focused transmitter," *IEEE Antennas Wireless Propag. Lett.*, vol. 18, no. 6, pp. 1105–1108, Jun. 2019, doi: 10.1109/LAWP.2019.2910200.

[31] J. Bae, H. Koo, H. Lee, W. Lim, W. Lee, H. Kang, K. C. Hwang, K.-Y. Lee, and Y. Yang, "High-efficiency rectifier (5.2 GHz) using a class-F Dickson charge pump," *Microw. Opt. Technol. Lett.*, vol. 59, no. 12, pp. 3018–3023, 2017, doi: 10.1002/mop.30862.

JONGSEOK BAE (Member, IEEE) was born in Suwon, South Korea, in 1987. He received the B.S. degree in electronic engineering from Chungnam University, Daejeon, South Korea, in 2014, and the Ph.D. degree from the Department of Electrical and Computer Engineering, Sungkyunkwan University, Suwon, in 2020.

Since 2020, he has been with the Department of Electrical and Computer Engineering, Sungkyunkwan University, where he is currently a Postdoctoral Fellow. His research interests include the design of RF/mm-wave power amplifiers, RF and analog integrated circuits, and microwave power transfer.

SANG-HWA YI (Member, IEEE) received the B.S. degree in electronic engineering from Korea University, Seoul, South Korea, in 2001, and the M.S. and Ph.D. degrees in microwave engineering from the Pohang University of Science and Technology (POSTECH), Pohang, South Korea, in 2003 and 2016, respectively.

Since 2013, he has been with the Korea Electro-technology Research Institute (KERI), South Korea, where he has been developed various electromagnetic partial-discharge sensors for diagnosis of power apparatuses, including gas-insulated-switchgears, transformers, and rotating machines. He is currently a Principal Researcher of the Power Grid Research Division, KERI. His research interest includes large-scale wireless power transfer via microwaves for space solar power satellite.

Dr. Yi is a member of the IEEE DEI–Society, the MTT-Society, and the AP-Society. He awarded Korean Minister of Trade, Industry and Energy's Commendation in invention day of 2020.

HYUNGMO KOO was born in Seoul, South Korea, in 1992. He received the B.S. degree from the Department of Electronic and Electrical Engineering, Sungkyunkwan University, Suwon, South Korea, in 2016. He is currently pursuing the Ph.D. degree with the Department of Electrical and Computer Engineering, Sungkyunkwan University.

His current research interests include the design of RF power amplifiers, efficiency enhancement techniques, transceiver arrays, microwave power transmission, and passive circuits optimizations.

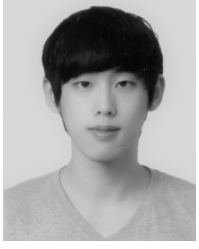

SUNGJAE OH was born in Gwangju, South Korea, in 1992. He received the B.S. degree from the Department of Electronic and Electrical Engineering, Sungkyunkwan University, Suwon, South Korea, in 2015. He is currently pursuing the Ph.D. degree with the Department of Electrical and Computer Engineering, Sungkyunkwan University.

His current research interests include the design of RF/mm-wave power amplifiers, analog integrated circuits, efficiency enhancement, broadband, and linearization techniques.

HANSIK OH was born in Seoul, South Korea, in 1991. He received the B.S. degree from the Department of Electronic and Electrical Engineering, Sungkyunkwan University, Suwon, South Korea, in 2016. He is currently pursuing the Ph.D. degree with the Department of Electrical and Computer Engineering, Sungkyunkwan University.

His current research interests include the design of RF power amplifiers, RF integrated circuits, analog integrated circuits, efficiency enhancement techniques, and linearization techniques.

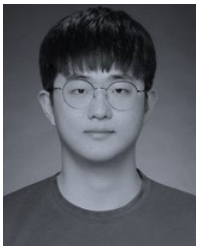

WOOJIN CHOI (Graduate Student Member, IEEE) was born in Kyunggi-do, South Korea, in 1993. He received the B.S. degree from the Department of Electronic and Electrical Engineering, Sungkyunkwan University, Suwon, South Korea, in 2016. He is currently pursuing the Ph.D. degree with the Department of Electrical and Computer Engineering, Sungkyunkwan University.

His current research interests include the design of RF/mm-wave power amplifiers, broadband techniques, and mm-wave integration circuits.

JAEKYUNG SHIN was born in Seoul, South Korea, in 1993. He received the B.S. degree from the Department of Electronic and Electrical Engineering, Korea Aerospace University, Goyang, South Korea, in 2018. He is currently pursuing the Ph.D. degree with the Department of Electrical and Computer Engineering, Sungkyunkwan University, Suwon, South Korea.

His current research interests include the design of RF/mm-wave power amplifiers, efficiency enhancement techniques, broadband techniques, and microwave power transmission.

CHAN MI SONG (Member, IEEE) received the B.S. degree in electronics and electrical engineering from Dongguk University, Seoul, South Korea, in 2015. She is currently pursuing the combined M.S. and Ph.D. degrees in electronic and electrical with Sungkyunkwan University, Suwon, South Korea.

Her research interests include microwave power transfer and array antenna design.

KEUM CHEOL HWANG (Senior Member, IEEE) received the B.S. degree in electronics engineering from Pusan National University, Busan, South Korea, in 2001, and the M.S. and Ph.D. degrees in electrical and electronic engineering from the Korea Advanced Institute of Science and Technology (KAIST), Daejeon, South Korea, in 2003 and 2006, respectively. From 2006 to 2008, he was a Senior Research Engineer with Samsung Thales, Yongin, South Korea, where he was involved with the development of various antennas including multiband fractal antennas for communication systems and Cassegrain reflector antenna and slotted waveguide arrays for tracking radars. From 2008 to 2014, he was an Associate Professor with the Division of Electronics and Electrical Engineering, Dongguk University, Seoul, South Korea. He joined the Department of Electronic and Electrical Engineering, Sungkyunkwan University, Suwon, South Korea, in 2015, where he is currently an Associate Professor. His research interests include advanced electromagnetic scattering and radiation theory and applications, design of multi-band/broadband antennas and radar antennas, and optimization algorithms for electromagnetic applications. He is a Life Member of KIEES and a member of IEICE.

KANG-YOON LEE (Senior Member, IEEE) received the B.S., M.S., and Ph.D. degrees from the School of Electrical Engineering, Seoul National University, Seoul, South Korea, in 1996, 1998, and 2003, respectively. From 2003 to 2005, he was with GCT Semiconductor Inc., San Jose, CA, USA, where he was a Manager of the Analog Division and worked on the design of CMOS frequency synthesizer for CDMA/PCS/PDC and single-chip CMOS RF chip sets for W-CDMA, WLAN, and PHS. From 2005 to 2011, he was an Associate Professor with the Department of Electronics Engineering, Konkuk University. Since 2012, he has been with College of Information and Communication Engineering, Sungkyunkwan University, South Korea, where he is currently an Associate Professor. His research interests include implementation of power integrated circuits, CMOS RF transceiver, analog integrated circuits, and analog/digital mixed-mode VLSI system design.

YOUNGOO YANG (Senior Member, IEEE) was born in Hamyang, South Korea, in 1969. He received the Ph.D. degree in electrical and electronic engineering from the Pohang University of Science and Technology, Pohang, South Korea, in 2002.

From 2002 to 2005, he was with Skyworks Solutions, Inc., Newbury Park, CA, USA, where he designed power amplifiers for various cellular handsets. Since 2005, he has been with the School of Information and Communication Engineering, Sungkyunkwan University, Suwon, South Korea, where he is currently a Professor. His current research interests include RF/mm-wave power amplifiers, RF transmitters, and dc-dc converters.